Interaction of two differently sized oscillating bubbles in a free field

Interaction of two differently sized oscillating bubbles in a free field

Lup Wai Chew,[1] Evert Klaseboer,[2] Siew-Wan Ohl,[2] and Boo Cheong Khoo[1,3,*]

[1]*Department of Mechanical Engineering, National University of Singapore, Kent Ridge, Singapore 119260*

[2]*Institute of High Performance Computing, 1 Fusionopolis Way, #16-16 Connexis, Singapore 138632*

[3]*Singapore-MIT Alliance, 4 Engineering Drive 3, Singapore 117576*

(Received 31 May 2011; revised manuscript received 15 August 2011; published 12 December 2011)

Most real life bubble dynamics applications involve multiple bubbles, for example, in cavitation erosion prevention, ultrasonic baths, underwater warfare, and medical applications involving microbubble contrast agents. Most scientific dealings with bubble-bubble interaction focus on two similarly sized bubbles. In this study, the interaction between two oscillating differently sized bubbles (generated in tap water) is studied using high speed photography. Four types of bubble behavior were observed, namely, jetting toward each other, jetting away from each other, bubble coalescence, and a behavior termed the "catapult" effect. In-phase bubbles jet toward each other, while out-of-phase bubbles jet away from each other. There exists a critical phase difference that separates the two regimes. The behavior of the bubbles is fully characterized by their dimensionless separation distance, their phase difference, and their size ratio. It is also found that for bubbles with large size difference, the smaller bubble behaves similarly to a single bubble oscillating near a free surface.

DOI: 10.1103/PhysRevE.84.066307 PACS number(s): 47.55.dd, 47.55.dr

I. INTRODUCTION

The understanding of oscillating (or nonequilibrium) bubble dynamics is fundamental and applicable to many physical phenomena ranging from cavitation on ship propellers to medical applications involving high intensity focused ultrasound. Direct observation of nonequilibrium bubbles is difficult due to their small sizes (typically submillimeter) and short oscillation period (in the order of milliseconds). Detailed studies of bubble dynamics revealing much of the underlying physics are now possible with the advancement in high speed photography technology.

A large number of bubble dynamics articles are based on the study of the oscillation of a single bubble in a free field by Lord Rayleigh [1]. The collapse of a single bubble in a free field is spherical and does not produce a liquid jet [2,3]. Gravity effects are negligible as the Froude number is very large (in the order of 10^3 [2]). When a solid boundary (e.g., a steel plate) is introduced near the oscillating bubble, it was shown in both simulation and experiment that the bubble will collapse with a liquid jet which directs toward the boundary [4–8]. On the other hand, the collapse of a single bubble near a free surface (e.g., water-air interface) will cause the development of a liquid jet which directs away from the free surface [9,10].

The behavior of two adjacent oscillating bubbles is complex, even if it is far away from a solid boundary or free surface [11,12]. Each of the bubbles may develop a jet. These jets can either direct toward or away from one another. Bubble coalescence may occur if the two (in-phase) bubbles are created very near to each other. Moreover, the size of the bubbles can be different and this adds another parameter to the analysis. Using a pulsed laser system, Lauterborn [13] studied the interaction between two similarly sized bubbles; while Lauterborn and Hentschel [14] studied the interaction between two differently sized bubbles. Other studies on the interaction of multiple bubbles can also be found in Blake *et al.* [15] and Tomita *et al.* [16]. Only a few cases are presented in both articles and no generalized graph is provided. A study on oscillating bubbles generated by reducing the ambient pressure rapidly on a hydrophobic surface with microcavities was presented by Bremond *et al.* [17,18]. The bubbles generated this way are always oscillating in phase. Other works on the behavior of multiple oscillating bubbles in the presence of imposed fluctuating pressure fields without jet formation can be found in Chatzidai *et al.* [19] and Ida [20].

The bubble-collapse-induced liquid jet can be used for several applications, including surface cleaning [21,22] and the removal of particles from holes [23]. Microbubbles are also used in biomedical fields such as cancer diagnosis [24] and drug delivery into biological cells by enhancing the permeability of the cell membrane [25]. Nevertheless, the liquid jet can be detrimental in some cases as it may cause cavitation erosion [26]. However, Brujan *et al.* [27] showed that the damage potential of the liquid jet can be minimized if the bubble nucleation point is fixed at a certain distance away from the solid surface.

Although there are several experimental and computational papers on multiple bubble interaction reported in the literature, there is a lack of works focusing on determining systematically and quantitatively the effect of bubble distance and phasing on the bubbles' behavior. Fong *et al.* [28] summarized the interaction between two similarly sized bubbles in a plot where the behavior of the bubbles can be predicted from the dimensionless separation distance and the phase difference between the two bubbles. The conditions leading to the development of four types of behavior of bubble-bubble interaction, namely, the (bubble-collapse-induced) liquid jets directed toward each other, liquid jets directed away from each other, bubble coalescence, and the so-called catapult effect are clearly demarcated in the plot. However, no such quantitative prediction of bubble dynamics is reported for differently sized bubbles in the literature. This paper aims to generalize the study of interaction of similarly sized bubbles to the interaction of differently sized bubbles in a free field. We describe the experimental setup in Sec. II, the interaction between two

*mpekbc@nus.edu.sg

similarly sized bubbles in Sec. III, and the interaction between two differently sized bubbles in Sec. IV. We present the parameters that govern the bubble behaviors in Sec. V. The results are given in Sec. VI and the conclusion follows in Sec. VII.

II. THE EXPERIMENTAL SETUP

The liquid used is tap water at room temperature. There are three common ways to generate oscillating bubbles in water: by laser, by acoustic wave [high intensity focused ultrasound (HIFU) or shock wave], or by spark discharge. The use of laser is advantageous as it is highly accurate in controlling the bubble nucleation spot and it is nonintrusive to the system, but the setup is rather complex and costly. HIFU can generate bubbles without disturbing the flow but the control of the nucleation spot is poor. The (low voltage) spark-discharge method adopted in this research has the advantages of being simple and low in cost [28–30]. This method can accurately control the bubble nucleation spot and is able to create multiple bubbles (of different sizes and at different locations) simultaneously. The major drawbacks are that the less precise control of the bubble size and the electrodes, which are immersed in the water, may cause interference to the ensuing bubble dynamics. To minimize possible interference, the electrodes used are very fine (0.2 mm in diameter) and the bubbles created have a maximum diameter of 20 times or larger (>4 mm) than the electrodes.

The schematic of the experimental setup is shown in Fig. 1. An acrylic water tank is filled to 90% with tap water. Two pairs of electrodes are used to generate two bubbles. The electrodes are fine copper wires held in place by acrylic pillars. The pillars are supported by a base which is fixed to the bottom of the tank. Both pairs of electrodes are placed in the middle of the tank and submerged 50% below the water level to eliminate wall and free surface effects. The electrodes are connected to the main circuit through insulated wires. To create the bubbles, two capacitors are fully charged to 60 V through a 1 kΩ resistor. The capacitors are then discharged by

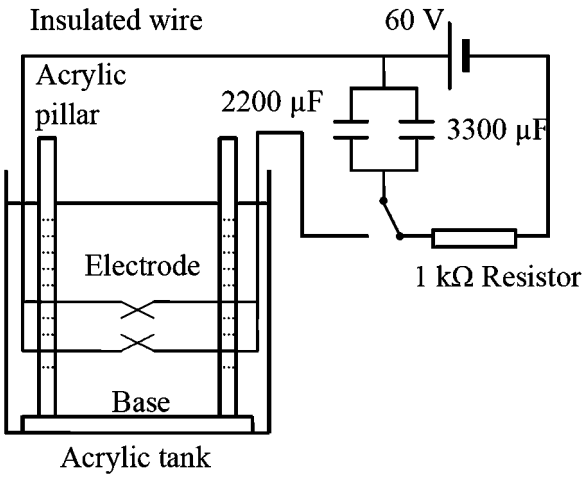

FIG. 1. The experimental setup consisting of a water tank with dimension 17 × 17 × 17 cm. Two parallel capacitors are charged with the 60 V power source. Through a two-way switch, the capacitors are then short-circuited through two pairs of electrodes to create two bubbles in the tank. The electrodes are touching each other.

short-circuiting them through the pair of crossed electrodes. The sparks from the discharged energy led to the creation of two gaseous bubbles. The oscillation period (the duration of the bubble from its first appearance until its collapse) of the bubble ranges between 0.4 and 2.0 ms, depending on the bubble size. The maximum bubble radius ranges between 2 and 7 mm. The charging voltage of 60 V is much lower than the voltage required for noncontact electrodes. For example, 8500 V was used in Blake and Gibson [31] and 4000 V was used in Buogo and Vokurka [32]. This makes the low voltage spark-discharge method an attractive alternative because it is safer to operate and lower in cost. The remnants of the burnt electrodes serve as black particles that aid flow visualization.

A high speed camera (Photron Fastcam SA1.1) is used to capture the bubble dynamics with a framing rate of 20 000 frames per second (shutter speed is between 1/20 000 and 1/56 000, aperture value of 8). A 250 W light source (Iwasaki Electric) located at the back (backlighting) is diffused through a piece of semitransparent filter paper.

III. INTERACTION OF TWO SIMILARLY SIZED BUBBLES

The spark-discharge method has less precise control over the bubble size (compared to the laser-induced bubble). The size of the bubble created is dependent on several factors, such as the area of contact of the crossing electrodes and the tightness of the winding of the electrodes onto the main wires. The electrodes will break after being short-circuited so they need to be replaced after every experiment. A new pair of electrodes may entail a different area of contact and as such, it is practically not possible to create two bubbles with exactly the same size. Therefore, all cases with size differences smaller than 15% are considered to have similar size. There are four major types of behavior that can be observed for two similarly sized bubbles: bubble coalescence, water jets directed toward each other, water jets directed away from each other, and the so-called catapult effect. Although similar results have been shown in the literature [13,28], the experiments on similarly sized bubbles are repeated to validate the experimental setup and to obtain more data for the plotting of summary graphs. Some typical examples are shown and discussed in this section.

A. On bubble coalescence

Figure 2 shows images captured using the high speed camera with each frame showing the elapsed time from the start of the first spark (taken to be $t = 0$) in milliseconds. Frame 1 shows two pairs of crossing electrodes with the length scale (10 mm black line). Bubble coalescence is observed for two in-phase bubbles that are created very near to each other. Both bubbles are created at $t = 0$ (frame 1) and continue to expand (frame 2) until the water film between them breaks presumably around $t = 0.40$ ms (frame 3). The coalesced bubble continues to expand as a single bubble (frame 4) until it reaches its maximum volume at $t = 0.65$ ms (frame 5). It is interesting to note that the coalesced bubble does not expand into a sphere but maintains its "hourglass" shape. It then starts to shrink and collapses into a disk (frame 6 to 8) to reach its minimum volume at $t = 1.10$ ms (frame 9). Frame 10 shows that no

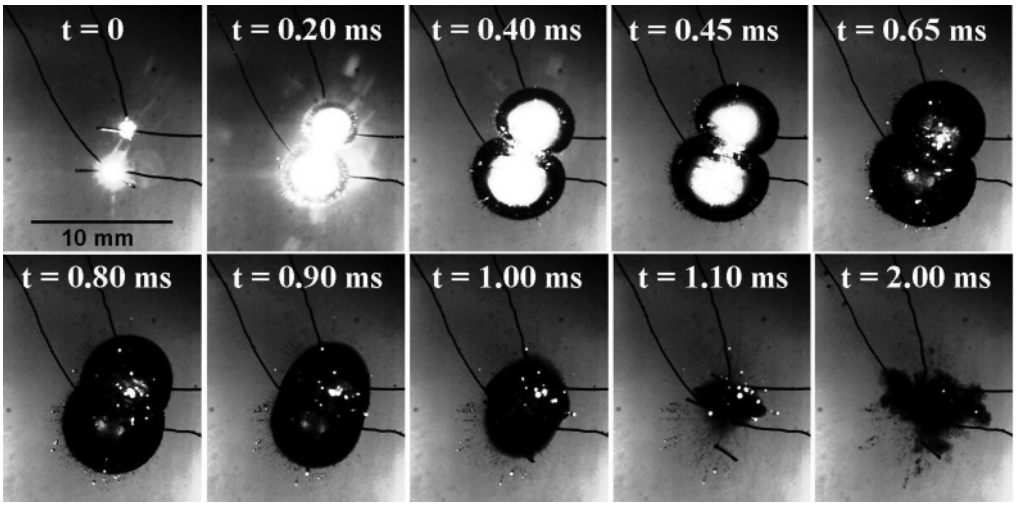

FIG. 2. Case 1, bubble coalescence for similarly sized bubbles ($R_{max,1} = 3.79$ mm; $R_{max,2} = 3.58$ mm; $d = 3.19$ mm; $t_{osc,1} = 1.1$ ms; $t_{osc,2} = 1.1$ ms; $\Delta t = 0$). The bubbles expand to their maximum sizes at $t = 0.65$ ms. At this time, the bottom bubble (bubble 2) is slightly larger than the top bubble (bubble 1). At around $t = 0.40$ ms the two bubbles merge and continue to oscillate as one bubble.

water jet is developed since the remnants of the bubbles stay stationary after the collapse of the coalesced bubble. The main bubble is seen to have broken up into many smaller bubbles.

B. On water jets directed toward each other

Two in-phase bubbles created far apart will develop two water jets that propagate toward each other, as shown in Fig. 3. Both bubbles are created at $t = 0$ (frame 1) and expand (frame 2) until bubble 2 (the bottom bubble) reaches its maximum volume at $t = 0.50$ ms (frame 3), followed by bubble 1 to reach its maximum volume at $t = 0.65$ ms (frame 4). Bubble 2 collapses at $t = 0.85$ ms (frame 5). At $t = 1.00$ ms (frame 6), bubble 1 collapses while the water jet developed from the collapse of bubble 2 is jetting toward bubble 1. Frames 7 and 8 show that remnants of the bubbles migrate toward each other, indicating that the water jets are directed toward each other after both bubbles have collapsed.

C. On water jets directed away from each other

Two out-of-phase bubbles tend to develop water jets directed away from each other. Both bubbles are created at the same time at $t = 0$ (frame 1), as shown in Fig. 4. Both bubbles continue to expand (frame 2) until bubble 1 (top bubble) reaches its maximum volume at $t = 0.70$ ms (frame 3). Bubble 1 then starts to shrink while bubble 2 is still expanding (frame 4). Bubble 1 collapses at $t = 1.10$ ms, exactly the same

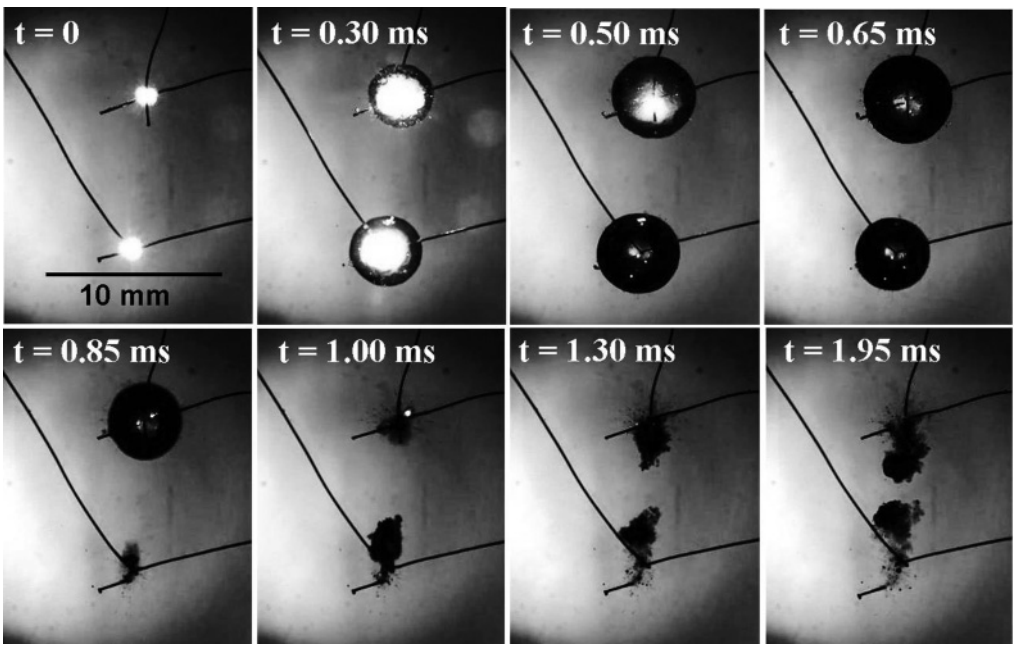

FIG. 3. Case 2, water jets directed toward each other for similarly sized bubbles ($R_{max,1} = 2.57$ mm; $R_{max,2} = 2.33$ mm; $d = 8.69$ mm; $t_{osc,1} = 1.0$ ms; $t_{osc,2} = 0.85$ ms; $\Delta t = 0$). The bottom bubble collapses first with an upward directed jet at $t = 0.85$ ms. This is followed shortly afterward by the upper bubble, which collapses with a downward jet at $t = 1.00$ ms. The bubbles are considered to be in phase.

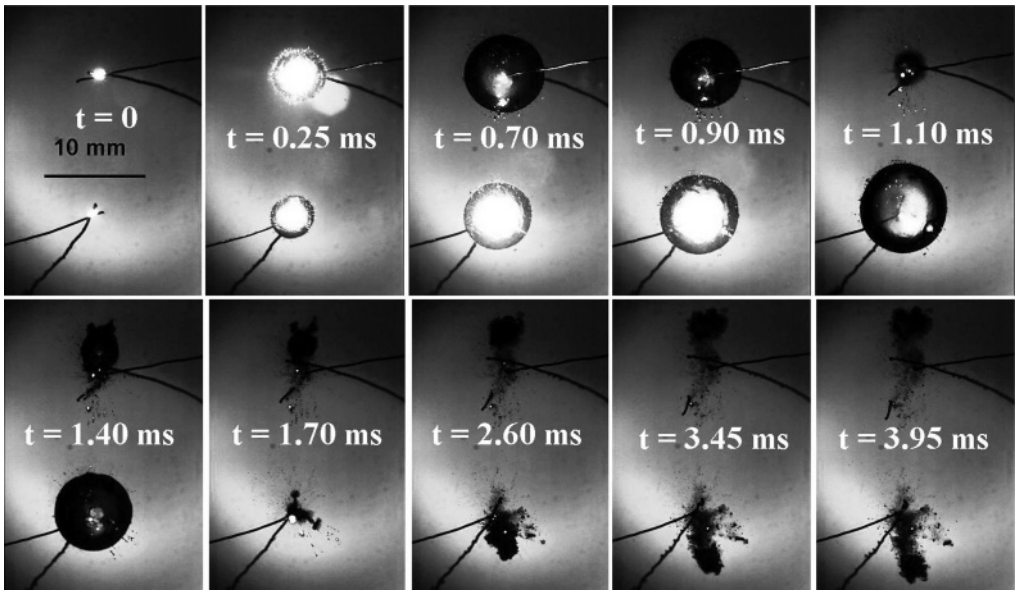

FIG. 4. Case 3, water jets directed away from each other for similarly sized bubbles ($R_{\max,1} = 4.24$ mm; $R_{\max,2} = 4.42$ mm; $d = 13.75$ mm; $t_{\text{osc},1} = 1.1$ ms; $t_{\text{osc},2} = 1.7$ ms; $\Delta t = 0$). The top bubble collapses at $t = 1.10$ ms with an upward directed jet (away from the bottom bubble). The bottom bubble collapses at $t = 1.70$ ms also developing a jet directed away from the top bubble. The bubbles are out of phase. Note the distinct difference in behavior when comparing to in-phase bubbles in case 2.

time when bubble 2 reaches its maximum volume (frame 5). Bubble 2 then begins to shrink while the water jet from the collapse of bubble 1 is jetting away from it (frame 6). Bubble 2 collapses at $t = 1.70$ ms (frame 7). Frames 8, 9, and 10 show that overall, the water jets propagate away from each other.

D. On the catapult effect

The catapult effect is a special case of water jets directed away from each other. In this case, the water jet developed by the collapse of bubble 2 (the second bubble created) is of much higher speed, up to the order of 10^2 m/s. The catapult effect is so named because bubble 1 (the first bubble created) seems to have supplied energy for bubble 2 by distorting it (analogous to the storing of elastic potential energy in a bow from the stretching of the string), and then releases the stored energy over a very short period of time when it collapses. This sudden "burst" of energy develops a very high speed jet (>50 m/s) that penetrates bubble 2.

Figure 5 shows an example of the catapult effect. Bubble 1 (the top bubble) is created at $t = 0$ (frame 1). Bubble 2 is created later at $t = 0.25$ ms (frame 2). Bubble 1 reaches its maximum volume at $t = 0.55$ ms while bubble 2 is still expanding (frame 3). The shape of bubble 2 is distorted as it protrudes into bubble 1 (frame 4). The maximum distortion is seen when bubble 1 reaches its minimum volume while bubble 2 reaches its maximum volume at $t = 1.05$ ms (frame 5). Bubble 2 then regains its spherical shape (frame 6) and this restoration in shape is believed to have developed a water jet that penetrates bubble 2. The tip of the water jet can be seen in the bubble in frame 6 and at the opposite side of bubble 2 in frame 7. The speed of the water jet can be estimated by measuring the distance traveled by the jet tip, then dividing that by the travel time. Referring to frames 6 and 7, and assuming that the water jet is created at $t = 1.15$ ms (frame 6), the tip of the jet has traveled 11.6 mm after 0.1 ms (at $t = 1.25$ ms, frame 7) so the average speed of the water jet is 116 m/s. The water jet is so powerful that it continues to propagate with an estimated speed of 32.8 m/s (calculated from the distance traveled by the jet tip from $t = 1.25$ ms to $t = 1.35$ ms).

The conditions leading to the generation of the catapult effect are very stringent: one of the bubbles must be at the phase near its minimum volume when the other bubble reaches its maximum volume. Moreover, the distance between the two bubbles must not be too small to avoid bubble coalescence; nor must it be too large such that the distortion on bubble 2 cannot be developed. Some cases resemble the catapult effect where the bubble shape distortion is observed but the strong water jet is not developed, such as the one presented next.

Figure 6 shows an example of the "failed catapult" effect. Both bubbles are created at $t = 0$ (frame 1) and expand (frame 2) until bubble 1 (top bubble) reaches its maximum size at $t = 0.95$ ms (frame 3). The expanding bubble 2 is distorted and protrudes into bubble 1. Some spiky protrusions are seen on the surface of bubble 2. The spiky instability is clearly seen at $t = 1.00$ ms (frame 4). Bubble 2 reaches its maximum volume at $t = 1.10$ ms (frame 5). The collapse of bubble 1 at $t = 1.30$ ms (frame 6) restores the spherical shape of bubble 2 (frames 7 and 8) until bubble 2 collapses at $t = 1.55$ ms (frame 9). The distortion on bubble 2 is expected to produce a high speed water jet that pierces through bubble 2 as observed in the catapult effect (as in Fig. 5). Frame 10, however, shows that no such high speed jet is developed as the remnants of the bubbles move away with a very low speed downward (about 2.6 m/s). It is postulated that the water jet in this so-called failed catapult either loses all its energy while penetrating the second bubble or the distortion on bubble 2 is not profound enough to create a high speed water jet. Another plausible cause could be the rupture of the water film between the two bubbles.

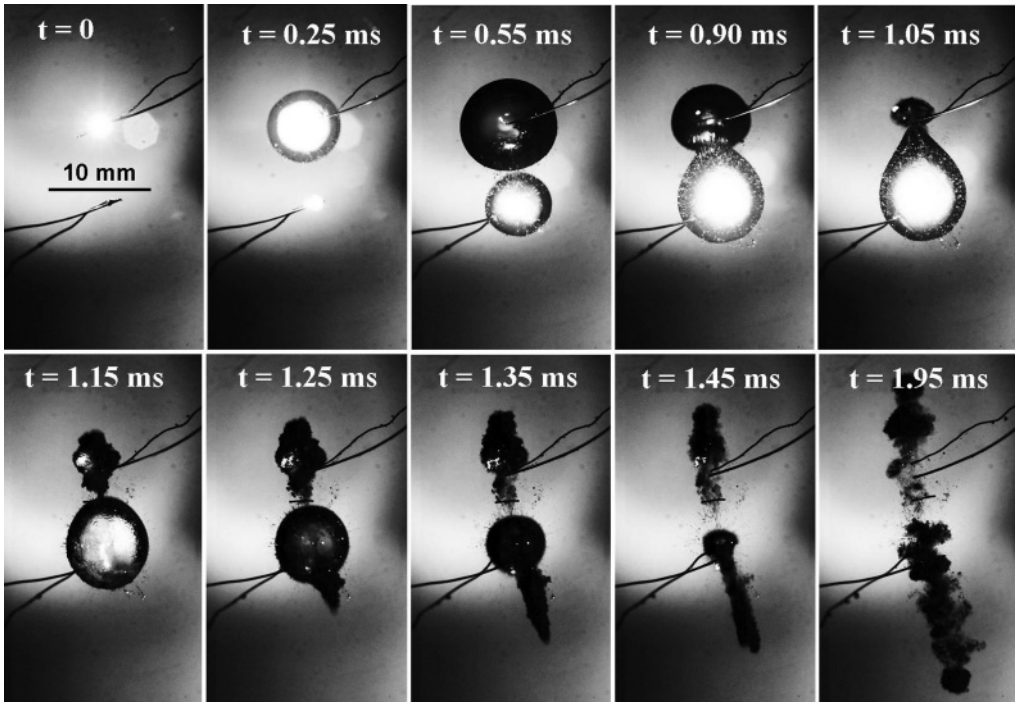

FIG. 5. Case 4, the catapult effect for similarly sized bubbles ($R_{\max,1} = 4.71$ mm; $R_{\max,2} = 4.20$ mm; $d = 7.56$ mm; $t_{\text{osc},1} = 1.05$ ms; $t_{\text{osc},2} = 1.2$ ms; $\Delta t = 0.25$ ms). The catapult effect only occurs for bubbles which are initiated very near to each other, and are out of phase. The bottom bubble is expanding while the upper bubble is in its collapse phase. This generates an elongated bottom bubble at $t = 1.05$ ms. The top bubble collapses, generating a jet that can be seen to traverse the bottom bubble at $t = 1.15$ ms. It impacts with a very high speed ($\sim$100 m/s) at $t = 1.25$ ms. Both bubbles jet away from each other.

IV. INTERACTION OF TWO DIFFERENTLY SIZED BUBBLES

So far, we have investigated the behavior of similarly sized bubbles, which is consistent (except for the failed catapult effect) with earlier literature [28]. In this section, two bubbles of different size are generated. The maximum bubble radius ranges from 2 to 7 mm, so the maximum size difference is 250%. Since all cases with bubble size difference <15% are considered to have similar size, "differently sized" bubbles are defined as any pair of bubbles with a size difference between 15% and 250%. Interestingly, all four major types of behavior (bubble coalescence, water jets directed away from each other, water jets directed toward each other, and the catapult effect) observed in the cases with similarly sized bubbles are also

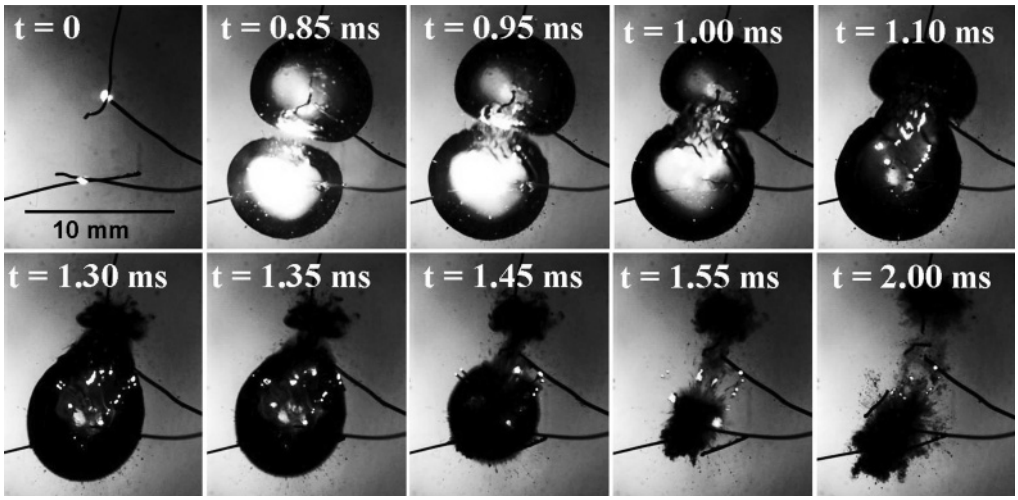

FIG. 6. Case 5, the failed catapult effect for similarly sized bubbles ($R_{\max,1} = 4.39$ mm; $R_{\max,2} = 4.28$ mm; $d = 5.82$ mm; $t_{\text{osc},1} = 1.30$ ms; $t_{\text{osc},2} = 1.55$ ms; $\Delta t = 0$). Compare this case to case 4. The reason for the failed catapult effect is not clear, but it may be that the bubbles coalesced around $t = 1.00$ ms and break up again around $t = 1.35$ ms, thereby preventing the catapult effect. The wavy surface ($t = 0.95$–1.10 ms) was also observed in bubble coalescence experiments of Fong *et al.* [28].

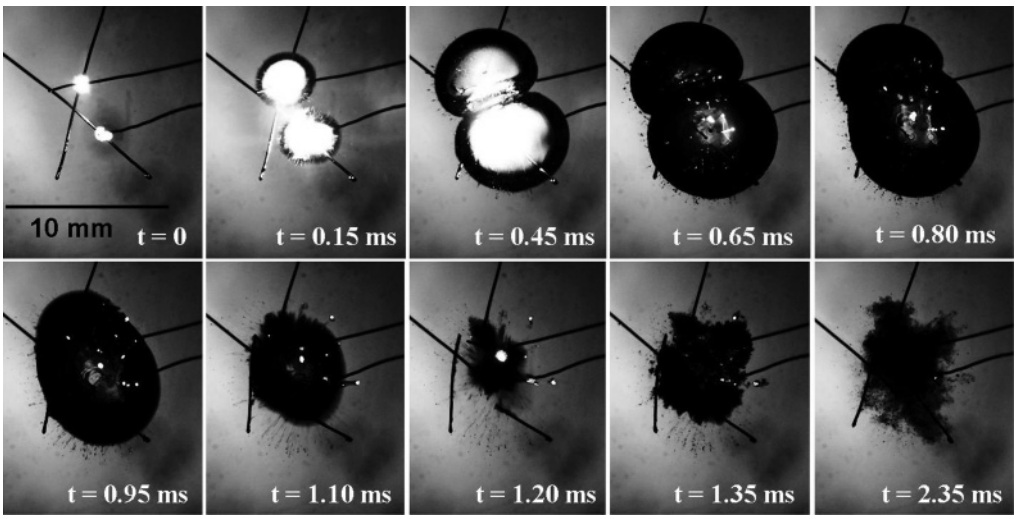

FIG. 7. Case 6, bubble coalescence for differently sized bubbles ($R_{\max,1} = 3.33$ mm; $R_{\max,2} = 4.13$ mm; $d = 3.48$ mm; $t_{\text{osc},1} = 1.2$ ms; $t_{\text{osc},2} = 1.2$ ms; $\Delta t = 0$). The top (smaller) bubble merges with the bottom (larger) bubble to form a single collapsing bubble. The behavior is very similar to case 1, but in this case an oval shaped bubble is formed from the coalesced bubbles ($t = 0.95$ ms).

observed in cases with differently sized bubbles. Some typical cases are shown in the next sections.

A. On bubble coalescence

For in-phase bubbles that are created very near to each other, bubble coalescence is observed, as shown in Fig. 7. Both bubbles are incepted simultaneously at $t = 0$ (frame 1) and expand (frame 2) until the water film between them breaks at $t = 0.45$ ms (frame 3). The coalesced bubble continues to expand while maintaining its hourglass shape (frame 4) and reaches its maximum size at $t = 0.80$ ms (frame 5). The coalesced bubble then collapses into a sphere (frames 6 and 7) and reaches its minimum volume at $t = 1.20$ ms (frame 8). Frames 9 and 10 show that two opposite water jets have developed in the coalesced bubble, consistent with the findings in Rungsiyaphornrat *et al.* [33].

B. On water jets directed toward each other

For in-phase bubbles created far apart from each other, two water jets directed toward each other are developed, as shown in Fig. 8. Both bubbles are created at $t = 0$ (frame 1), and continue to expand (frame 2) until bubble 2 reaches its maximum volume at $t = 0.65$ ms (frame 3). Bubble 1 reaches its maximum volume at $t = 0.90$ ms while bubble 2 is shrinking (frame 4). Bubble 2 and bubble 1 reach their minimum volume at $t = 1.00$ ms (frame 5) and $t = 1.40$ ms (frame 7), respectively. Frames 8, 9, and 10 show that the water jets developed from the collapse of both bubbles propagate toward each other.

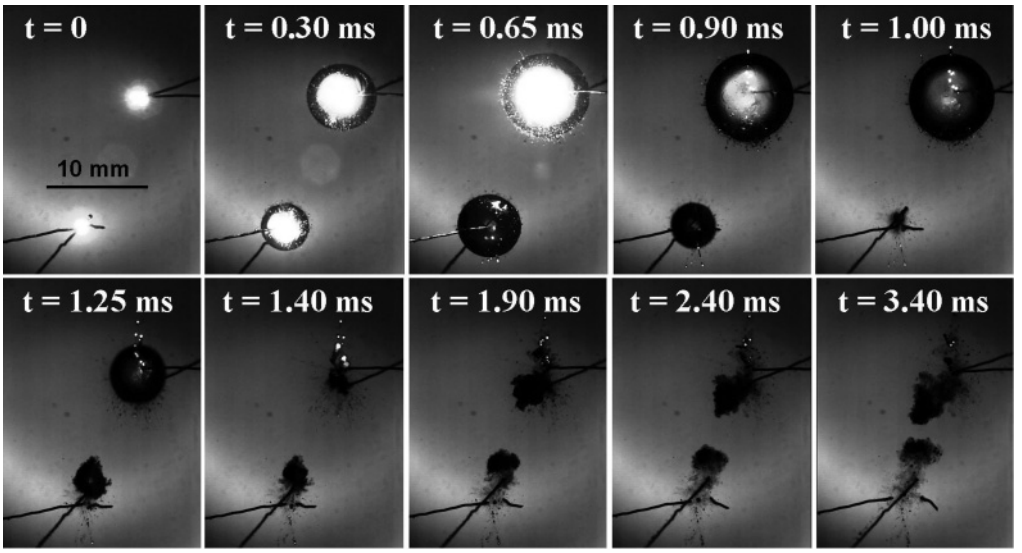

FIG. 8. Case 7, water jets directed toward each other for differently sized bubbles ($R_{\max,1} = 4.44$ mm; $R_{\max,2} = 2.95$ mm; $d = 13.89$ mm; $t_{\text{osc},1} = 1.4$ ms; $t_{\text{osc},2} = 1.0$ ms; $\Delta t = 0$). The bottom (smaller) bubble collapses first at $t = 1.00$ ms with a jet toward the top (larger) bubble. The larger bubble collapses at $t = 1.40$ ms developing a jet directed toward the lower bubble. The observed behavior is very similar to case 2.

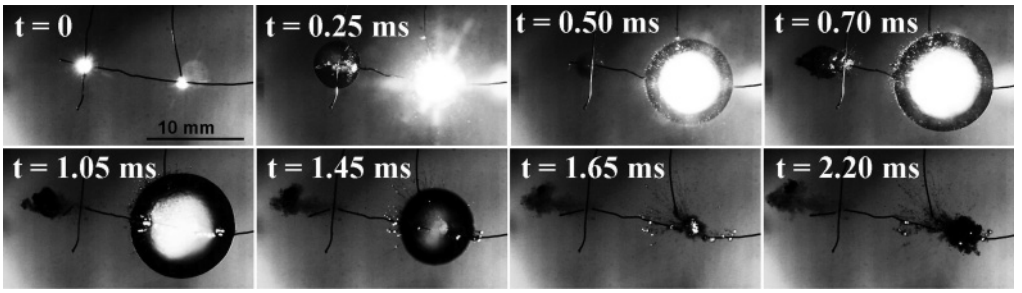

FIG. 9. Case 8, water jets directed away from each other for differently sized bubbles ($R_{max,1} = 2.48$ mm; $R_{max,2} = 5.28$ mm; $d = 10.24$ mm; $t_{osc,1} = 0.5$ ms; $t_{osc,2} = 1.65$ ms; $\Delta t = 0$). The left (smaller) bubble collapses while the right (larger) bubble is still expanding as in case 3. Note that the remnants of the bubble and electrodes act as flow tracer particles for the bubble on the right-hand side.

C. On water jets directed away from each other

For out-of-phase bubbles, two liquid jets directed away from each other are observed. Figure 9 shows that both bubble 1 and bubble 2 are created at $t = 0$ (frame 1). Bubble 1 reaches its maximum volume at $t = 0.25$ ms (frame 2) and collapses at $t = 0.50$ ms while bubble 2 is still expanding (frame 3). The collapse of bubble 1 develops a water jet directed away from bubble 2 (frame 4). Bubble 2 then reaches its maximum volume at $t = 1.05$ ms while the jet from the collapse of bubble 1 continues to move away (frame 5). Bubble 2 then shrinks (frame 6) and reaches its minimum volume at $t = 1.65$ ms (frame 7). Frame 8 shows that the water jet developed from the collapse of bubble 2 is directed away from the jet of bubble 1. Hence it is concluded that the two water jets propagate away from each other.

D. On the catapult effect

The intriguing catapult effect is also observed in cases for differently sized bubbles, as shown in Fig. 10. Bubble 1 is created at $t = 0$ (frame 1) and expands (frame 2, note that the bright spot at the right-hand side is a reflection and should not be mistaken for a spark) until bubble 2 is created at $t = 0.40$ ms (frame 3), hence the time difference, $\Delta t = 0.40$ ms. Bubble 1 then reaches its maximum volume at $t = 0.60$ ms while bubble 2 is expanding (frame 4). The expanding bubble 2 protrudes into the shrinking bubble 1 (frames 5, 6, 7, 8, and 9) until bubble 1 collapses at $t = 1.15$ ms and bubble 2 regains its spherical shape (frame 10). Bubble 2 collapses at $t = 1.60$ ms and the water jet developed is directed away from the remnants of bubble 1 (frame 11). The water jet speed at this frame is estimated to be 60 m/s.

As observed for the similarly sized bubbles, the conditions for the development of the catapult effect are very restrictive for the differently sized bubbles. The distance from the adjacent bubble must be perfectly positioned to avoid bubble coalescence, yet close enough so that the shape distortion on the second bubble can occur. Some of the cases fail to develop the strong water jet although the conditions seem to match. Figure 11 shows an example of this failed catapult with distortion on bubble 2 but the high speed water jet is not developed. The trajectory of the remnants of the bubbles proves that the speed of the water jet is very low (<10 m/s). The range of conditions for the successful generation of the catapult effect is much more restrictive compared to the other three modes (to be shown in Sec. VI). When successfully generated, it is expected that the high speed water jet developed from the catapult effect could be very useful in applications involving water jets such as surface cleaning.

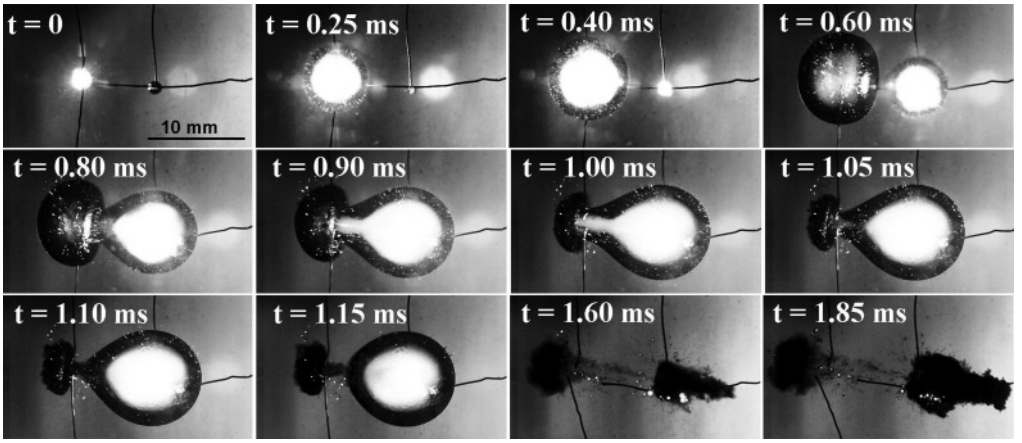

FIG. 10. Case 9, the catapult effect for differently sized bubbles ($R_{max,1} = 4.36$ mm; $R_{max,2} = 5.33$ mm; $d = 7.70$ mm; $t_{osc,1} = 1.15$ ms; $t_{osc,2} = 1.2$ ms; $\Delta t = 0.4$ ms). The bubble on the right is being sucked in by the collapsing bubble on the left from $t = 0.80$–1.05 ms. Upon its own collapse, the bubble at the right generates a very high speed jet towards the right-hand side. The behavior is remarkably similar to the one of case 4.

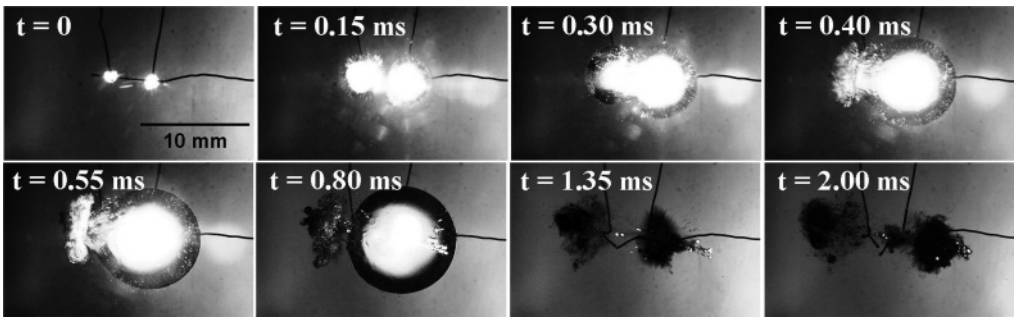

FIG. 11. Case 10, the failed catapult effect for differently sized bubbles ($R_{max,1} = 2.76$ mm; $R_{max,2} = 5.31$ mm; $d = 3.84$ mm; $t_{osc,1} = 0.40$ ms; $t_{osc,2} = 1.35$ ms; $\Delta t = 0$). As in case 5, the interface of the left bubble gets corrugated at $t = 0.40$ ms to $t = 0.55$ ms; possibly the bubbles have merged during this stage. They are clearly separated again at $t = 0.80$ ms. Two opposite jets still occur, but with much less velocity than in case 9.

V. DIMENSIONLESS PARAMETERS GOVERNING THE BUBBLE BEHAVIOR

Because of the complexities of the behavior of differently sized bubbles, we shall adopt dimensionless parameters to characterize the bubble behavior. Several important parameters that govern the behavior of a two-bubble interaction as shown in Figs. 12 and 13 are (i) the distance between the two bubbles, d; (ii) the maximum radius of each bubble, $R_{max,1}$ and $R_{max,2}$; (iii) the oscillation period (duration from bubble nucleation till bubble collapse) of each bubble, $t_{osc,1}$ and $t_{osc,2}$; (iv) the elapsed time from the moment of bubble nucleation until the moment when one of the bubbles collapses to its minimum volume, t_1 and t_2; and (v) the inception time difference, Δt.

Subscript 1 denotes bubble 1, while subscript 2 denotes bubble 2. In Figs. 2–11, the parameters are indicated in the caption for each case. Note that the medium used (tap water) is assumed to be inviscid so the viscosity is not included in the dimensional analysis. For very small bubbles viscosity can become important (see Versluis *et al.* [34]). Surface tension effects are considered to be negligible as the Weber number is in the order of 10^3 [33,35]. The effect of gravity is also negligible as the Froude number is in the order of 10^3, ten times larger than the critical value of 130 [2]. In essence, the behavior of the bubble is a function of all the above parameters:

$$\text{Bubble behavior} = f(d, R_{max,1}, R_{max,2}, t_1, t_2, t_{osc,1}, t_{osc,2}, \Delta t). \quad (1)$$

From careful observation of many experiments, for both similarly sized and differently sized bubbles, the corresponding dimensionless parameters deemed critical are the dimensionless separation distance (γ), the phase difference ($\Delta\theta$), and the size difference ratio (S). The nondimensional separation distance between the bubbles is defined as

$$\gamma = \frac{d}{R_{max,1} + R_{max,2}}. \quad (2)$$

With this definition, at $\gamma = 1$, the two bubbles are touching each other if they were solid spheres. The phase difference is defined as

$$\Delta\theta = \left| \left(\frac{t_1}{t_{osc,1}} - \frac{t_2}{t_{osc,2}} \right) \right| + \frac{\Delta t}{t_{osc,1}}. \quad (3)$$

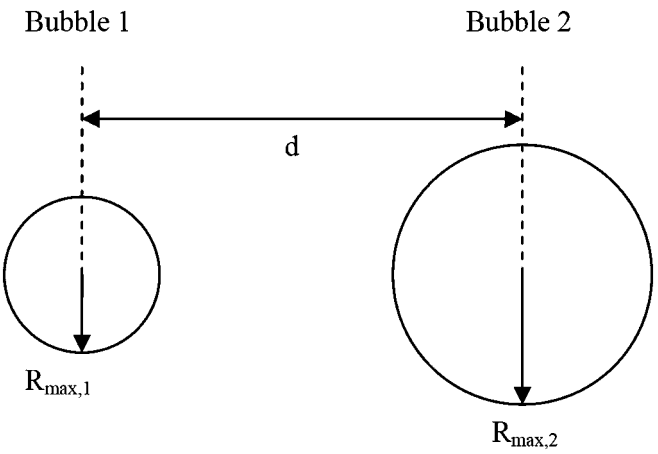

FIG. 12. Definition of $R_{max,1}$, $R_{max,2}$, and d.

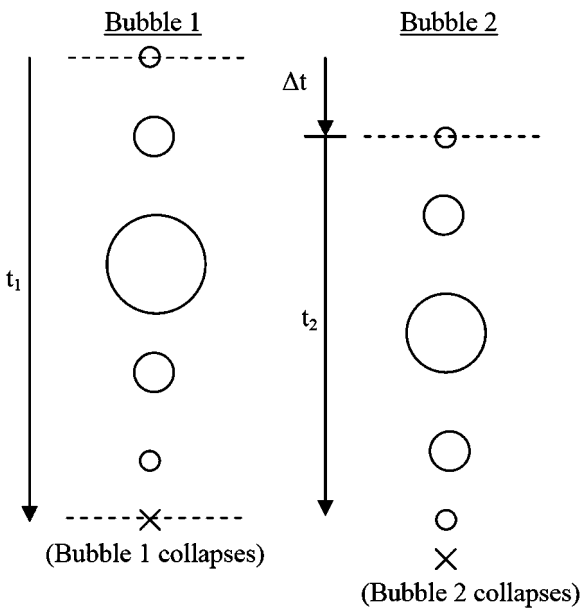

FIG. 13. Definition of t_1, t_2, and Δt.

Bubble 1 is taken literally as the first bubble to be created. If two bubbles are created at the same time ($\Delta t = 0$), either bubble can be taken as bubble 1. "Completely in-phase" bubbles are defined to have $\Delta\theta = 0$, while "completely out-of-phase" bubbles have $\Delta\theta = 1$. In addition, the maximum ratio of $\Delta t/t_{\mathrm{osc},1}$ is limited to 0.5 so that the second bubble is always created before the first bubble reaches its maximum volume. This limitation is to ensure that the maximum $\Delta\theta$ does not exceed 1. Note that the present $\Delta\theta$ is defined slightly different from Fong *et al.* [28] in which

$$\Delta\theta' = 2\pi \left| \left(\frac{t_1}{t_{\mathrm{osc},1}} - \frac{t_2}{t_{\mathrm{osc},2}} \right) \right|. \tag{4}$$

The ratio of size difference is defined as

$$S = \frac{R_{\mathrm{max,L}}}{R_{\mathrm{max,S}}}. \tag{5}$$

Two bubbles with exactly the same size have $S = 1$. Since bubble 1 is defined as the first bubble created, either bubble 1 or bubble 2 can be the larger bubble. To keep $S \geqslant 1$, the radius of the larger bubble is divided by the radius of the smaller bubble (L denotes larger, while S denotes smaller in Eq. (5)). Therefore, $S = R_{\mathrm{max},2}/R_{\mathrm{max},1}$ if $R_{\mathrm{max},2} > R_{\mathrm{max},1}$ or $S = R_{\mathrm{max},1}/R_{\mathrm{max},2}$ if $R_{\mathrm{max},1} > R_{\mathrm{max},2}$.

VI. RESULTS AND DISCUSSION

For all cases (similarly sized and differently sized), the behavior of the bubble interaction is plotted into graphs with the dimensionless distance (γ) as the horizontal axis and the phase difference ($\Delta\theta$) as the vertical axis.

The experimental results for similarly sized bubbles are shown in Fig. 14. The conditions to develop the four major types of behavior are plotted (water jets directed away from each other, water jets directed toward each other, bubble coalescence, and the catapult effect). Each type of behavior occupies a distinct region in the graph with no overlapping of data points. From the graph, the water jets are directed

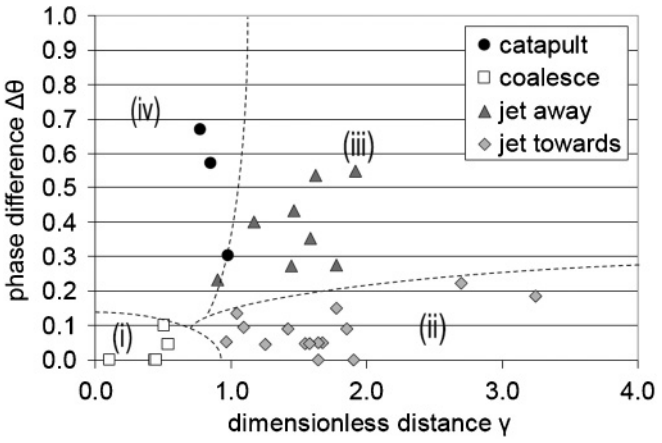

FIG. 14. Experimental result for similarly sized bubbles. Four distinct regions occur: (i) in phase, nearby bubbles coalesce; (ii) in-phase bubbles far away from each other develop water jets toward each other; (iii) out-of-phase bubbles that are far apart develop water jets away from each other; and (iv) out of phase, nearby bubbles develop the catapult effect.

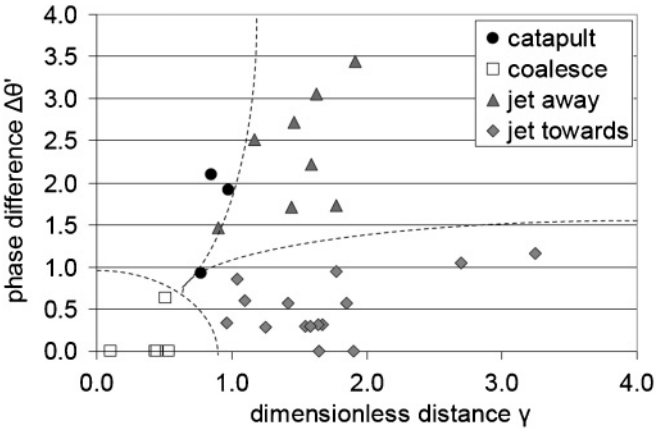

FIG. 15. Experimental result for similarly sized bubbles by using $\Delta\theta'$ formula as in Fong *et al.* [28].

toward each other when $\Delta\theta < 0.2$ and away from each other when $\Delta\theta > 0.2$. By definition, in-phase bubbles develop water jets directed toward each other whereas out-of-phase bubbles develop water jets directed away from each other. It can thus be concluded that the critical $\Delta\theta$ value to determine the phasing of the bubbles is about 0.2. Bubble coalescence occurs when $\gamma \leqslant 0.6$ and only if the bubbles are oscillating in phase, whereas the catapult effect is observed only for out-of-phase bubbles that have $\gamma < 1$ and $\Delta\theta > 0.3$. We have also plotted another graph by using $\Delta\theta'$ calculated from Eq. (4) given in Fong *et al.* [28] to compare our results to their results. Figure 15 shows that our results agree very well with the graph in Fong *et al.* [28] (not shown here). However, Eq. (4) cannot be used to calculate the phase difference between differently sized bubbles because the difference in their oscillation period is large, causing $\Delta\theta$ [using Eq. (4)] to exceed 2π, which is deemed unreasonable. Furthermore, we found that the factor π is not needed; hence we modified Eq. (4) into Eq. (3) for the calculation of $\Delta\theta$.

Figure 16 shows the plot for differently sized bubbles using the same parameters (γ and $\Delta\theta$). The bubble collapse tends to develop water jets toward each other when $\Delta\theta < 0.45$ or away from each other when $\Delta\theta > 0.45$ so the critical $\Delta\theta$ value that determines the phasing of the bubbles (in phase or out of phase) is about 0.45. On the other hand, bubble coalescence takes place when $\gamma < 0.6$ and $\Delta\theta < 0.1$ and the catapult effect occurs only when $\gamma < 1$ and $\Delta\theta > 0.7$.

Figures 14 and 16 show that the critical $\Delta\theta$ separating the jet away region from the jet toward region are 0.2 for similarly sized bubbles and 0.45 for differently sized bubbles. This deviation in critical $\Delta\theta$ value suggests that the size difference, S, has an effect in determining the behavior of the interacting bubbles. (One can always construe that S serves as the third dimension perpendicular to Fig. 14 or Fig. 16, and S varies from 1.0 to 1.15 in Fig. 14, while Fig. 16 essentially "lumped" all the data with values of S larger than 1.15.) In order to study the influence of S on the bubble's behavior, the graph of $\Delta\theta$ against S is plotted as shown in Fig. 17. Note that $S = 1.0$ corresponds to same sized bubbles. The graph S against γ is also plotted (not shown here) and we found that S is independent with respect to γ (as expected since the separation distance has no direct influence on the size of the bubbles). Thus Fig. 17 includes data points for all values of γ.

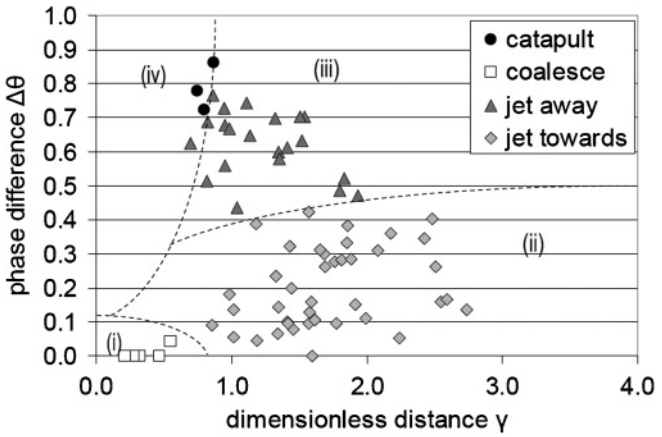

FIG. 16. Experimental result for differently sized bubbles. Four distinct regions occur: (i) in phase, nearby bubbles coalesce; (ii) in-phase bubbles far from each other develop water jets toward each other; (iii) out-of-phase bubbles that are far apart develop water jets away from each other; and (iv) out of phase, nearby bubbles develop the catapult effect.

Figure 17 shows that when S increases, the $\Delta\theta$ value required for "jetting away" to occur also increases. It is fairly clear and distinct that a demarcation can be drawn to separate the jet away region from the jet toward region. The demarcation starts at $\Delta\theta \approx 0.2$ when $S = 1$. We also know that as $S \to \infty$, bubble 1 becomes infinitely larger than bubble 2. As such, $R_{\max,1} \to \infty$ and the curvature ($= 1/R_{\max,1}$) of the surface of bubble 1 is zero. Zero curvature means bubble 1 resembles a water-gas free surface, and bubble 2 can thus be considered to be oscillating near a free surface. From the fact that $\Delta\theta = 1$ for a bubble oscillating near a free surface, the demarcation should therefore lead to $\Delta\theta = 1$ as $S \to \infty$. The curve fitting satisfying the above mentioned conditions at $S = 1$ and $S = \infty$ suggests a simple demarcation of the form

$$(\Delta\theta)_{\text{demarcation}} \approx \left(1 - \frac{1}{S + 0.25}\right). \tag{6}$$

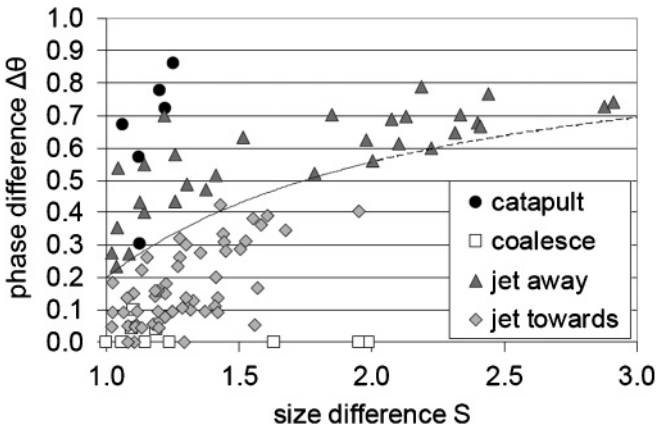

FIG. 17. Graph of phase difference against size difference. The catapult effect is observed only when $S < 1.3$; bubble coalescence and the jet toward behavior are observed only when $S < 2.0$; the jet away behavior is observed for all values of S.

This demarcation curve is shown in Fig. 17. $(\Delta\theta)_{\text{demarcation}}$ can be used to predict the direction of the water jet at any value of S: the water jets will be directed away from each other if $\Delta\theta > (\Delta\theta)_{\text{demarcation}}$ or directed toward each other if $\Delta\theta < (\Delta\theta)_{\text{demarcation}}$.

In addition, for $S > 2$, the water jet is always directed away from the other bubble (no cases of jetting toward each other are observed). This means that two bubbles with $S > 2$ always oscillate out of phase since only out-of-phase bubbles can develop water jets away from each other. As long as the large bubble is at least twice as large as the small bubble, the smaller bubble will perceive the large bubble as essentially a free surface and always develops a water jet away from the large bubble.

Another interesting feature inferred from Fig. 17 is that the catapult effect occurs only when $S < 1.3$. In other words, two bubbles with sufficiently large size difference have not been observed to generate the catapult effect. A possible reason is that the catapult effect can only be generated if one of the bubbles is at its maximum size, while the other bubble collapses, as discussed in Sec. III D. The phase difference required cannot be realized if S is too large because the large bubble (which has a much larger t_{osc}) is still at its early phase of expansion and has not reached its maximum size when the small bubble collapses. Another plausible explanation is that the small bubble is unable to significantly distort the shape of the large bubble due to their large difference in size.

VII. CONCLUSION

Two interacting spark-created bubbles (of similar and different size) are studied with high speed photography. Four types of behavior (bubble coalescence, water jets directed toward each other, water jets directed away from each other, and the catapult effect) are observed. The behavior of the oscillating bubbles is governed by the interbubble distance, the phase difference, and the size difference between the two bubbles. It is found that there are four well-defined regions in the graphs corresponding to the four types of bubble behavior. Bubbles located relatively far away from each other develop two water jets that are either directed toward each other (for in-phase bubbles) or away from each other (for out-of-phase bubbles). Bubbles located near to each other either coalesce (for in-phase bubbles) or develop the catapult effect (for out-of-phase bubbles). The graphs show consistency between similarly and differently sized bubbles as long as the size difference ratio is smaller than 2. The catapult effect is observed only for two bubbles with small size difference (<30%). If the large bubble is twice or larger in size than the small bubble, the small bubble behaves like a bubble oscillating near a free surface.

ACKNOWLEDGMENT

The authors would like to acknowledge the Impact Mechanics Lab at the National University of Singapore for the use and help in the setting up of the high speed photography system.

[1] Rayleigh, Philos. Mag. **34**, 94 (1917).
[2] C. K. Turangan, G. P. Ong, E. Klaseboer, and B. C. Khoo, J. Appl. Phys. **100**, 054910 (2006).
[3] A. Prosperetti, J. Acoust. Soc. Am. **101**, 2003 (1997).
[4] W. Lauterborn and H. Bolle, J. Fluid Mech. **72**, 391 (1975).
[5] A. Vogel, W. Lauterborn, and R. Timm, J. Fluid Mech. **206**, 299 (1989).
[6] J. R. Blake, M. C. Hooton, P. B. Robinson, and R. P. Tong, Philos. Trans. R. Soc. London, Ser. A **355**, 537 (1997).
[7] Y. L. Zhang, K. S. Yeo, B. C. Khoo, and C. Wang, J. Comput. Phys. **166**, 336 (2001).
[8] E. Klaseboer, K. C. Hung, C. Wang, C. W. Wang, B. C. Khoo, P. Boyce, S. Debono, and H. Charlier, J. Fluid Mech. **537**, 387 (2005).
[9] J. R. Blake and D. C. Gibson, Annu. Rev. Fluid Mech. **19**, 99 (1987).
[10] Q. X. Wang, K. S. Yeo, B. C. Khoo, and K. Y. Lam, Comput. Fluids **25**, 607 (1996).
[11] N. A. Pelekasis and J. A. Tsamopoulos, J. Fluid Mech. **254**, 467 (1993).
[12] N. A. Pelekasis and J. A. Tsamopoulos, J. Fluid Mech. **254**, 501 (1993).
[13] W. Lauterborn, Appl. Sci. Res. **38**, 165 (1982).
[14] W. Lauterborn and W. Hentschel, Ultrasonics **23**, 260 (1985).
[15] J. R. Blake, P. B. Robinson, A. Shima, and Y. Tomita, J. Fluid Mech. **255**, 707 (1993).
[16] Y. Tomita, A. Shima, and K. Sato, Appl. Phys. Lett. **57**, 234 (1990).
[17] N. Bremond, M. Arora, S. M. Dammer, and D. Lohse, Phys. Fluids **18**, 121505 (2006).
[18] N. Bremond, M. Arora, C. D. Ohl, and D. Lohse, Phys. Rev. Lett. **96**, 224501 (2006).
[19] N. Chatzidai, Y. Dimakopoulos, and J. Tsamopoulos, J. Fluid Mech. **673**, 513 (2011).
[20] M. Ida, Phys. Rev. E **79**, 016307 (2009).
[21] C. D. Ohl, M. Arora, R. Dijkink, V. Janve, and D. Lohse, Appl. Phys. Lett. **89**, 074102 (2006).
[22] W. D. Song, M. H. Hong, B. Lukyanchuk, and T. C. Chong, J. Appl. Phys. **95**, 2952 (2004).
[23] D. Pavard, E. Klaseboer, S. W. Ohl, and B. C. Khoo, Phys. Fluids **21**, 083304 (2009).
[24] M. Hwang, K. J. Niermann, A. Lyshchik, and A. C. Fleischer, Ultrasound Q. **25**, 175 (2009).
[25] N. Nomikou and A. P. McHale, Cancer Lett. **296**, 133 (2010).
[26] E. A. Brujan, K. Nahen, P. Schmidt, and A. Vogel, J. Fluid Mech. **433**, 251 (2001).
[27] E. A. Brujan, G. S. Keen, A. Vogel, and J. R. Blake, Phys. Fluids **14**, 85 (2002).
[28] S. W. Fong, D. Adhikari, E. Klaseboer, and B. C. Khoo, Exp. Fluids **46**, 705 (2009).
[29] K. S. F. Lew, E. Klaseboer, and B. C. Khoo, Sens. Actuators, A **133**, 161 (2007).
[30] M. Muller and P. Zima, *Proceedings of the WIMRC 3rd International Cavitation Forum 2011* (University of Warwick, United Kingdom, 2011), Paper 1B-8.
[31] J. R. Blake and D. C. Gibson, J. Fluid Mech. **111**, 123 (1981).
[32] S. Buogo and K. Vokurka, J. Sound Vib. **329**, 4266 (2010).
[33] S. Rungsiyaphornrat, E. Klaseboer, B. C. Khoo, and K. S. Yeo, Comput. Fluids **32**, 1049 (2003).
[34] M. Versluis, D. E. Goertz, P. Palanchon, I. L. Heitman, S. M. van der Meer, B. Dollet, N. de Jong, and D. Lohse, Phys. Rev. E **82**, 026321 (2010).
[35] Z. Y. Zhang and H. S. Zhang, Phys. Rev. E **71**, 066302 (2005).